

Symmetry Breaking in Symmetric Tensor Decomposition

Yossi Arjevani
New York University

Joan Bruna
New York University

Michael Field
UC Santa Barbara

Joe Kileel
University of Texas at Austin

Matthew Trager
Amazon*

Francis Williams
New York University

Abstract

In this note, we consider the optimization problem associated with computing the rank decomposition of a symmetric tensor. We show that, in a well-defined sense, minima in this highly nonconvex optimization problem break the symmetry of the target tensor—but not too much. This phenomenon of *symmetry breaking* applies to various choices of tensor norms, and makes it possible to study the optimization landscape using a set of recently-developed symmetry-based analytical tools. The fact that the objective function under consideration is a multivariate polynomial allows us to apply symbolic methods from computational algebra to obtain more refined information on the symmetry breaking phenomenon.

We consider the problem of approximating a given symmetric tensor as a sum of rank-1 symmetric tensors. Concretely, given an order n symmetric tensor $T \in \text{Sym}^n(\mathbb{R}^d)$ and a rank $k \in \mathbb{N}$, we aim to find good minimizers for the nonconvex optimization problem

$$\min_{W \in M(k,d)} \mathcal{L}(W), \quad \text{where } \mathcal{L}(W) := \left\| \sum_{i=1}^k \mathbf{w}_i^{\otimes n} - T \right\|^2. \quad (1)$$

Here, $M(k, d)$ denotes the space of all $k \times d$ matrices, $\|\cdot\|$ is some tensor norm and \mathbf{w}_i denotes the i -th row of W .¹ The problem of finding a tensor approximation of bounded rank arises naturally in various scientific fields, including machine learning, biomedical engineering and psychometrics. We refer the reader to [1, 2, 3, 4, 5, 6, 7] and references therein for a survey of relevant applications.

A natural approach for tackling (1) is to use local optimization methods, in particular gradient descent (GD) algorithms. However, as the optimization landscape associated with (1) is highly nonconvex, local methods can fail due to various geometric obstructions such as spurious minima (non-global local minima) and saddles. It is therefore desirable to obtain a good understanding of critical points of different extremal qualities. Although this goal may appear to be hopeless for generic nonconvex landscapes,² a recent line of works [10, 11, 12] showed that—in the presence of symmetry—a precise analytic characterization can be

*This work was performed prior to joining Amazon.

¹Note that for odd-order tensors, problem (1) is equivalent to the standard tensor rank decomposition (also known as the *real symmetric canonical polyadic decomposition (CPD)*). Treatment of even-order tensors, where any linear combination of rank-1 tensors is allowed, is deferred to future work.

²For approaches for studying *random* nonconvex landscapes see, e.g., [8, 9].

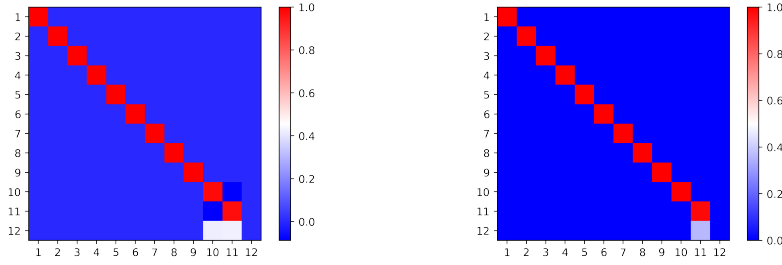


Figure 1: Spurious minima of optimization problem (1) instantiated with $d = k = 12$, order 3 symmetric tensors, the Frobenius norm (equivalently, the *cubic kernel* $\langle \cdot, \cdot \rangle^3$, as defined in (7)), and the target tensor $T = \sum_{i=1}^k \mathbf{e}_i^{\otimes 3}$. Symmetry of matrices in $M(k, d)$ is measured via the *isotropy groups* of a suitably-defined group action (see Section 2 for a formal exposition). (Left) a 12×12 -spurious minimum of isotropy $\Delta(S_9 \times S_2 \times S_1)$. The corresponding function value is $1/2$. (Right) a 12×12 -spurious minimum of isotropy $\Delta(S_{10} \times S_2)$. The corresponding function value is $1/2$.

obtained for families of critical points, as well as their Hessian spectrum. The premise of the approach is that the critical points of interest, such as those associated to spurious minima, break the symmetry of the target tensor T (measured by a suitable group of symmetries, see Section 2)—but not too much. Such critical points are called *symmetry breaking*.

In this note, we empirically demonstrate that the rich symmetry of (1) yields symmetry breaking spurious minima that lie on low-dimensional subspaces, which are determined by the structure of the target tensor T . For example, for $T = \sum_{i=1}^k \mathbf{e}_i^{\otimes 3}$, minima detected empirically using GD are shown to be symmetry breaking with respect to T (see Figure 1). Other choices of tensor norms and target tensors yield different types of symmetry breaking (see Section 3). Lastly, since \mathcal{L} is a multivariate polynomial, we are able to study symmetry breaking subspaces using tools from computational algebra—tools which that were not applicable in previous contexts in which the symmetry breaking phenomenon was studied.

Our contributions in order of appearance may be stated as follows:

- We formulate the invariance properties of optimization problems associated with symmetric tensor decomposition, and make their dependence on the target tensor explicit. Our analysis considerably generalizes the argument employed in [10] and applies to a wider class of *kernel-like* problems.
- We provide numerical results which demonstrate that minima tend to conform with the symmetry of the target tensor. In our experiments, we consider optimization problem (1) with the Frobenius inner product of order 3 and order 5 symmetric tensors, and the inner product associated with the standard Gaussian distribution (see Equation 14). We also examine different structural assumptions on the target tensors.
- A property of the symmetry breaking principle specific to symmetric tensor decomposition problems is that, unlike previous settings to which this principle applies [10], here \mathcal{L} is a multivariate polynomial. This makes it possible to use methods from computational algebra, for example Gröbner bases, which allow us to analytically characterize the set of highly-symmetric critical points to a large extent.

The note is organized as follows. In [Section 1](#), we review relevant notions from multilinear algebra and group actions to be used throughout the note. In [Section 2](#), we formally establish the invariance properties of \mathcal{L} with respect to various choices of inner products and target tensors. Lastly, in [Section 3](#) we present numerical experiments that explore the principle of symmetry breaking in different tensorial settings.

1 Preliminaries

Below, we provide background material for concepts and terms in multilinear algebra and group actions which are needed for a formal study of the symmetry breaking phenomenon in [problem \(1\)](#).

1.1 Tensor preliminaries

A tensor of order n is an element of the tensor product of n vector spaces $V_1 \otimes \dots \otimes V_n$. Upon choosing bases for each factor V_i , we may identify a tensor with a multi-dimensional array in $\mathbb{R}^{d_1 \times \dots \times d_n}$ (assuming V_i are real vector spaces) with $d_i = \dim(V_i)$. We write T_{i_1, \dots, i_n} for the (i_1, \dots, i_n) -th coordinate of T . Given vectors $\mathbf{v}_i \in \mathbb{R}^{d_i}$, $i = 1, \dots, n$, we write $\mathbf{v}_1 \otimes \dots \otimes \mathbf{v}_n$ for the outer product of these vectors, that is, the element in $\mathbb{R}^{d_1} \otimes \dots \otimes \mathbb{R}^{d_n}$ such that $(\mathbf{v}_1 \otimes \dots \otimes \mathbf{v}_n)_{i_1, \dots, i_n} = (v_1)_{i_1} \dots (v_n)_{i_n}$. Also, we write $\mathbf{v}^{\otimes n} := \mathbf{v} \otimes \dots \otimes \mathbf{v}$ (n -times). The Frobenius inner product of two tensors T, S of the same shape is defined to be $\langle T, S \rangle_F = \sum_{i_1, \dots, i_n} T_{i_1 \dots i_n} S_{i_1 \dots i_n}$. We will also consider other inner products of tensors. It is easy to see that for the Frobenius inner product we have

$$\langle \mathbf{v}_1 \otimes \dots \otimes \mathbf{v}_n, \mathbf{w}_1 \otimes \dots \otimes \mathbf{w}_n \rangle_F = \prod_{i=1}^n \langle \mathbf{v}_i, \mathbf{w}_i \rangle \quad (2)$$

for all $\mathbf{v}_i, \mathbf{w}_i \in \mathbb{R}^{d_i}$ ($i = 1, \dots, n$). In particular, $\langle \mathbf{v}^{\otimes n}, \mathbf{w}^{\otimes n} \rangle_F = \langle \mathbf{v}, \mathbf{w} \rangle^n$.

A tensor $T \in \mathbb{R}^d \otimes \dots \otimes \mathbb{R}^d$ (n times) is *symmetric* if it is invariant under permutation of indices, that is, if $T_{i_1, \dots, i_n} = T_{i_{\sigma(1)}, \dots, i_{\sigma(n)}}$ holds for all permutation $\sigma \in S_n$, where S_n is the symmetric group of degree n . We write $\text{Sym}^n(\mathbb{R}^d)$ for the space of symmetric tensors of order n on \mathbb{R}^d . This is a vector space of dimension $\binom{d+n-1}{n}$. It is isomorphic to the space of homogeneous polynomials of degree n in formal variables $\mathbf{X} = (X_1, \dots, X_d)$ via $T \mapsto \langle T, \mathbf{X}^{\otimes n} \rangle$. When $n = 2$, this is the usual correspondence between symmetric matrices and quadric forms. Finally, we recall the definition of *rank* for symmetric tensors. We say that $T \in \text{Sym}^n(\mathbb{R}^d)$ has rank-1 if $T = \lambda \mathbf{v}^{\otimes n}$ for some $\lambda \in \mathbb{R} \setminus \{0\}$ and $\mathbf{v} \in \mathbb{R}^d \setminus \{0\}$. More generally, a tensor T has (real symmetric) rank- r if it can be written as a linear combination of r rank-1 tensors $T = \lambda_1 \mathbf{v}_1^{\otimes n} + \dots + \lambda_k \mathbf{v}_k^{\otimes n}$, but not as a combination of $k - 1$ rank-1 tensors. For $n = 2$, this definition agrees with the usual notion of rank for symmetric matrices. In this note, we are interested in symmetric tensors of odd order. Thus, the coefficients λ_i may be absorbed into the vectors \mathbf{v}_i and dropped altogether. Let us briefly mention some current algorithms for symmetric tensor decomposition, that is, [problem \(1\)](#) when $\|\cdot\|$ is Frobenius. A straightforward yet practical method is based on direct first-order optimization of \mathcal{L} in [\(1\)](#); see [\[13\]](#) and the Matlab implementations [\[14, 15\]](#). A more computationally intensive although provable method (assuming T is rank r and $r = O(n^{\frac{d-1}{2}})$) was provided in [\[16\]](#), based on an algebraic construction called generating polynomials. For $n = 3$ and $r \leq d$, a classic but theoretically convenient method was derived from simultaneous diagonalization of matrix slices [\[17\]](#). For $n = 4$ and $r = O(n^2)$, the work [\[18\]](#) presented a provable algorithm using matrix eigendecompositions, which was robustified using ideas from the sums-of-squares hierarchy in [\[19\]](#). In [\[20\]](#), a tensor power method was used, constructed from a matrix flattening of T , to find the components \mathbf{w}_i sequentially. Also, [\[21\]](#) showed how to implement direct optimization of [\(1\)](#) in an efficient manner for moment tensors T in an online setting.

1.2 Groups, actions and symmetry

We review background material on group actions (see [22, Chapters 1, 2] for a more complete account). Elementary concepts from group theory are assumed known. We start with an example that is used later.

Example 1. Let $\text{GL}(d)$ denote the set of invertible linear maps on \mathbb{R}^d . Under composition, $\text{GL}(d)$ is a group, called the *general linear group*. The *orthogonal group* $\text{O}(d)$ is the subgroup of $\text{GL}(d)$ that preserves Euclidean distances, i.e., $\text{O}(d) = \{A \in \text{GL}(d) : \|Ax\|_2 = \|x\|_2 \text{ for all } x \in \mathbb{R}^d\}$. Upon choosing a basis for \mathbb{R}^d , both $\text{GL}(d, \mathbb{R})$ and $\text{O}(d)$ can be viewed as groups of invertible $d \times d$ matrices.

Group actions. Groups often arise as *transformations* of a set or space, so we are led to the notion of a *G-space* X where we have an *action* of a group G on a set X . Formally, a group action is a group homomorphism from G to the group of bijections of X . For example, S_d naturally acts on $[d] := \{1, \dots, d\}$ as the group of permutations, while both $\text{GL}(d)$ and $\text{O}(d)$ act on \mathbb{R}^d as groups of linear transformations (or matrix multiplication).

Example 2. Our study of the invariance properties of \mathcal{L} will rely on the action of the product group $S_k \times S_d \subseteq S_{k \times d}$ ($k, d \in \mathbb{N}$) on the product set $[k] \times [d]$ defined by

$$(\pi, \rho)(i, j) := (\pi^{-1}(i), \rho^{-1}(j)) \text{ for all } (\pi, \rho) \in S_k \times S_d, (i, j) \in [k] \times [d]. \quad (3)$$

By identifying $(i, j) \in [k] \times [d]$ with the entry (i, j) -entry in a matrix, this induces a linear representation on the space $M(k, d)$ of real $k \times d$ matrices $A = (A_{ij})$ via

$$(\pi, \rho)(A_{ij}) := (A_{\pi^{-1}(i), \rho^{-1}(j)}). \quad (4)$$

Here, π acts by permuting the rows of A , and ρ by permuting the columns of A . In terms of permutation matrices $P_\pi \in O(k)$ where

$$(P_\pi)_{ij} = \begin{cases} 1 & i = \pi(j), \\ 0 & \text{otherwise,} \end{cases}$$

and $P_\rho \in O(d)$ given similarly, the action is $(\pi, \rho)(A) = P_\pi A P_\rho^\top$.

Isotropy groups. Given $W \in M(k, d)$, the largest subgroup of $S_k \times S_d$ fixing W is called the *isotropy subgroup* (or *stabilizer*) of W and is used as a means of measuring the symmetry of W . The isotropy subgroup of $I_d \in M(d, d)$ is the diagonal subgroup ΔS_d , where Δ maps a given subgroup $H \subseteq S_d$ to its *diagonal* counterpart $\{(g, g) : g \in H\} \subseteq S_d \times S_d$ (thus, a transposition (ij) in ΔS_k acts by simultaneously switching the i th and j th rows and columns). The *fixed point space* corresponding to a given subgroup $H \subseteq G$ is defined to be

$$M(k, d)^H = \{W \in M(k, d) : hW = W \forall h \in H\}.$$

This is a linear subspace of $M(k, d)$. In [Section 3.1](#), we consider spurious minima whose isotropy groups are subgroups of the isotropy group of the identity tensor $\tau_n(I_k)$, e.g., $\Delta S_d, \Delta(S_{d-1} \times S_1)$ (see [Figure 2](#)) and $\Delta(S_{d-3} \times S_2 \times S_1)$. [Section 3.3](#) addresses other choices of target matrices and different symmetry breaking patterns (see also [10]).

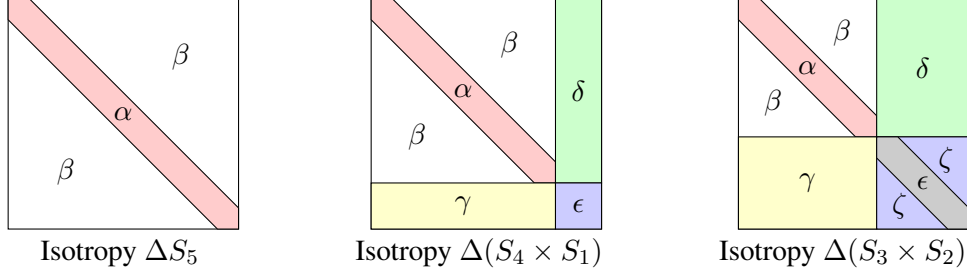


Figure 2: A schematic description of 5×5 matrices with isotropy ΔS_5 , $\Delta(S_4 \times S_1)$ and $\Delta(S_3 \times S_2)$, from left to right (borrowed from [10]). $\alpha, \beta, \gamma, \delta, \epsilon$ and ζ are assumed to be ‘sufficiently’ different.

2 Invariance properties of the loss function

In the sequel, we formally establish the invariance properties of problem (1). We further show that the same analysis applies in fact to a kernel-like formulation of a greater generality, and use this observation to study the symmetry breaking phenomenon in related settings. We conclude the section with a brief discussion of a recent symmetry-based approach [10, 11, 12] which allows one to exploit invariance properties of nonconvex functions to analyze the associated optimization landscape.

A real-valued function f with domain X is G -invariant if $f(g\mathbf{x}) = f(\mathbf{x})$ for all $\mathbf{x} \in X$, $g \in G$. Let us regard the loss function \mathcal{L} for symmetric tensor decomposition in (1) as a function on the $S_k \times S_d$ -space $M(k, d)$ (see Example 2). Since permuting the order of the summation in (1) does not change the function value, \mathcal{L} is left S_k -invariant (i.e., invariant under row permutations of W) for all choices of T . Additional invariance properties of \mathcal{L} may exist depending on the structure of the target tensor T . To see this, we define the map τ_n on matrices $A \in M(k, n)$ as follows

$$\tau_n(A) := \sum_{i=1}^k \mathbf{a}_i^{\otimes n}, \quad (5)$$

where $\mathbf{a}_1, \dots, \mathbf{a}_k$ are the rows of the matrix A . Next, we make the definition of \mathcal{L} explicit with respect to the target tensor (by a slight abuse of notation):

$$\mathcal{L}(W; V) := \|\tau_n(W) - \tau_n(V)\|^2, \quad (6)$$

where $V \in M(h, d)$ and $T = \tau_n(V)$. Note that \mathcal{L} is left S_h -invariant with respect to its second argument, where S_h is understood as acting by permuting the rows of V . Moreover, we no longer regard the target tensor T in problem (1) as a primary object in our analysis, but rather, shift attention to its parameterization—the target weight matrix V .

Specializing the norm $\|\cdot\|$ to be the one induced by the Frobenius inner product, (6) takes the form:

$$\begin{aligned}
\mathcal{L}(W; V) &= \langle \tau_n(W) - \tau_n(V), \tau_n(W) - \tau_n(V) \rangle_F \\
&= \sum_{i,j=1}^k \langle \mathbf{w}_i^{\otimes n}, \mathbf{w}_j^{\otimes n} \rangle_F - 2 \sum_{i=1}^k \sum_{j=1}^h \langle \mathbf{w}_i^{\otimes n}, \mathbf{v}_j^{\otimes n} \rangle_F + \sum_{i,j=1}^h \langle \mathbf{v}_i^{\otimes n}, \mathbf{v}_j^{\otimes n} \rangle_F \\
&= \sum_{i,j=1}^k \langle \mathbf{w}_i, \mathbf{w}_j \rangle_F^n - 2 \sum_{i=1}^k \sum_{j=1}^h \langle \mathbf{w}_i, \mathbf{v}_j \rangle_F^n + \sum_{i,j=1}^h \langle \mathbf{v}_i, \mathbf{v}_j \rangle_F^n. \tag{7}
\end{aligned}$$

Since $\langle \cdot, \cdot \rangle^n$ is rotationally invariant, it follows that $\mathcal{L}(W; V) = \mathcal{L}(WU; VU)$ for all $U \in O(d)$. Assuming momentarily that $h = d$ and $V = I_d$, we have for all $(\pi, \rho) \in S_k \times S_d$:

$$\mathcal{L}(W) = \mathcal{L}(W; I_d) = \mathcal{L}(W; P_\rho P_\rho^\top) = \mathcal{L}(W P_\rho; P_\rho) = \mathcal{L}(P_\pi W P_\rho; I_d) = \mathcal{L}(P_\pi W P_\rho). \tag{8}$$

Thus, \mathcal{L} is $S_k \times S_d$ -invariant for the choice of $V = I_d$. More generally, if $V \in M(h, d)$, $\sigma \in S_h$, $\rho \in S_d$ are such that $V P_\rho = P_\sigma V$, then

$$\mathcal{L}(W) = \mathcal{L}(W; V) = \mathcal{L}(W P_\rho; V P_\rho) = \mathcal{L}(W P_\rho; P_\sigma V) = \mathcal{L}(W P_\rho; V) = \mathcal{L}(W P_\rho). \tag{9}$$

Note that the condition $V P_\rho = P_\sigma V$ is actually expressing that $\tau_n(V P_\rho) = \tau_n(V)$ (see also Lemma 4 below). The relation (9) shows that symmetries of the target tensor lead to invariance properties of the objective function. For example, if $V \in M(d, d)$ is a *circulant matrix*, then $V P_\rho = P_\rho V$ holds for any *cyclic* permutation $\rho \in S_d$. Thus, (9) implies that $\mathcal{L}(W) = \mathcal{L}(P_\pi W P_\rho)$ for all permutations $\pi \in S_k$ (as left S_k -invariance always holds) and all cyclic $\rho \in S_d$, giving an $S_k \times \mathbb{Z}_d$ -invariance of \mathcal{L} . We shall address a special case of circulant matrices in Section 3.3.

The kernel-like formulation (10) suggests a simple way of considerably relaxing the use of the Frobenius norm while maintaining the $S_k \times S_d$ -invariance. Indeed, replacing $\langle \cdot, \cdot \rangle^n$ by a general *kernel* $\kappa(\cdot, \cdot)$, (7) reads as follows:

$$\mathcal{L}_\kappa(W; V) := \sum_{i,j=1}^k \kappa(\mathbf{w}_i, \mathbf{w}_j)_F^n - 2 \sum_{i=1}^k \sum_{j=1}^h \kappa(\mathbf{w}_i, \mathbf{v}_j)_F^n + \sum_{i,j=1}^h \kappa(\mathbf{v}_i, \mathbf{v}_j)_F^n. \tag{10}$$

Throughout the note, we assume that κ is invariant under a simultaneous right multiplication of both arguments by orthogonal matrices, yielding an $S_k \times S_d$ -invariance of \mathcal{L}_κ using the same line of argument above. This yields a straightforward, yet effective, generalization of the invariance analysis given in [10, Section 4.1]. In particular, an important example of an $O(d)$ -invariant kernel comes from the study of shallow ReLU neural networks [10, 11]:

$$\begin{aligned}
\kappa(\mathbf{w}, \mathbf{v}) &:= \mathbb{E}_{\mathbf{x} \sim \mathcal{N}(0, I_d)} [\max\{\langle \mathbf{w}, \mathbf{x} \rangle_F, 0\} \max\{\langle \mathbf{v}, \mathbf{x} \rangle_F, 0\}] \\
&= \frac{1}{2\pi} \|\mathbf{w}\|_2 \|\mathbf{v}\|_2 (\sin(\theta_{\mathbf{w}, \mathbf{v}}) + (\pi - \theta_{\mathbf{w}, \mathbf{v}}) \cos(\theta_{\mathbf{w}, \mathbf{v}})), \tag{11}
\end{aligned}$$

where $\theta_{\mathbf{w}, \mathbf{v}} := \cos^{-1} \left(\frac{\langle \mathbf{w}, \mathbf{v} \rangle_F}{\|\mathbf{w}\|_2 \|\mathbf{v}\|_2} \right)$. More generally, the class of $O(d)$ -invariant kernels includes any random-features model [23] of the form $k(\mathbf{w}, \mathbf{v}) = \mathbb{E}_{\mathbf{x} \sim \nu} [\rho(\langle \mathbf{w}, \mathbf{x} \rangle) \rho(\langle \mathbf{v}, \mathbf{x} \rangle)]$ with an activation function ρ and an $O(d)$ -invariant distribution ν . The functions κ and ρ are related through their spherical harmonic decompositions (one being the square of the other).

In particular, $O(d)$ -invariant kernels are induced by probability distributions over \mathbb{R}^d [24]. Given such a probability distribution \mathcal{D} , we define an inner product of tensors by letting

$$\langle S, T \rangle_{\mathcal{D}} := \mathbb{E}_{\mathbf{x} \sim \mathcal{D}}[\langle S, \mathbf{x}^{\otimes n} \rangle_F \langle T, \mathbf{x}^{\otimes n} \rangle_F], \quad (12)$$

which in turn induces the kernel $k(\mathbf{w}, \mathbf{v}) = \langle \tau_n(\mathbf{w}), \tau_n(\mathbf{v}) \rangle_{\mathcal{D}}$.³ The inner product $\langle \cdot, \cdot \rangle_{\mathcal{D}}$ can be explicitly expressed in terms of the $2n$ -moments of \mathcal{D} as follows.

Lemma 3. For tensors $S, T \in \text{Sym}^n(\mathbb{R}^d)$, we have that

$$\langle S, T \rangle_{\mathcal{D}} = \text{vec}(S)^\top \text{mat}(\mathbf{M}_{\mathcal{D}, 2n}) \text{vec}(T) \quad (13)$$

where $\mathbf{M}_{\mathcal{D}, 2n} := \mathbb{E}_{\mathbf{x} \sim \mathcal{D}}[\mathbf{x}^{\otimes 2n}] \in \text{Sym}^{2n}(\mathbb{R}^d)$ is the $2n$ -th moment tensor of \mathcal{D} , and vec and mat are the linear operators of vectorization and matricization with respect to lexicographic ordering.⁴

Proof We compute

$$\begin{aligned} \langle S, T \rangle_{\mathcal{D}} &:= \mathbb{E}_{\mathbf{x} \sim \mathcal{D}}[\langle S, \mathbf{x}^{\otimes n} \rangle_F \langle T, \mathbf{x}^{\otimes n} \rangle_F] \\ &= \mathbb{E}_{\mathbf{x} \sim \mathcal{D}}[\langle S \otimes T, \mathbf{x}^{\otimes 2n} \rangle_F] \\ &= \langle S \otimes T, \mathbb{E}_{\mathbf{x} \sim \mathcal{D}} \mathbf{x}^{\otimes 2n} \rangle_F \\ &= \langle S \otimes T, \mathbf{M}_{\mathcal{D}, 2n} \rangle_F \\ &= \text{vec}(S)^\top \text{mat}(\mathbf{M}_{\mathcal{D}, 2n}) \text{vec}(T), \end{aligned} \quad (14)$$

using properties of tensor product and the linearity of expectation. This gives the result. ■

The way by which different choices of $\mathbf{M}_{\mathcal{D}, 2n}$ affect the optimization landscape of problem (1) is studied in [24]. Here, we shall only consider the *cubic-Gaussian kernel* corresponding to the third-order inner-product induced by the standard Gaussian distribution,

$$k(\mathbf{w}, \mathbf{v}) = 6\langle \mathbf{w}, \mathbf{v} \rangle_F^3 + 9\|\mathbf{w}\|_2^2 \|\mathbf{v}\|_2^2 \langle \mathbf{v}, \mathbf{w} \rangle_F. \quad (15)$$

We note in passing that an alternative interpretation for the ‘‘partially symmetric tensors’’ we consider is that of *partially symmetric* homogeneous polynomials. This is formulated by the following lemma.

Lemma 4. Let $G \subseteq S_d$ be a subgroup. Assume $V \in M(h, d)$ is such that for each $\rho \in G$ there exists $\sigma \in S_h$ such that $VP_\rho = P_\sigma V$. Let $T = \tau_n(V)$ correspond to the homogeneous polynomial F of degree n in variables $\mathbf{X} = (X_1, \dots, X_d)$ via $F = \langle T, \mathbf{X}^{\otimes n} \rangle$. Then F is a G -invariant where S_d acts by permutation of variables.

Proof For each permutation $\rho \in G \subseteq S_d$, we have that $\rho F = \langle T, (\rho \mathbf{X})^{\otimes n} \rangle_F = \langle T, \rho^{\otimes n} \mathbf{X}^{\otimes n} \rangle_F = \langle (\rho^{-1})^{\otimes n} \tau_n(V), \mathbf{X}^{\otimes n} \rangle_F = \langle \tau_n(V P_{\rho^{-1}}), \mathbf{X}^{\otimes n} \rangle_F = \langle \tau_n(P_\sigma V), \mathbf{X}^{\otimes n} \rangle_F = \langle \tau_n(V), \mathbf{X}^{\otimes n} \rangle_F = F$, where we used the fact that $\tau_n(P_\sigma V) = \tau_n(V)$. ■

Thus, in the language of homogeneous polynomials, by considering problem (1) with structured targets T , we are studying the *Waring decompositions* of partially symmetric homogeneous polynomials [7].

³It can be shown that the Frobenius inner product is not induced by any probability distribution [24].

⁴In Matlab notation, $\text{vec}(T) = \text{reshape}(T, d^n)$ and $\text{mat}(\mathbf{M}) = \text{reshape}(\mathbf{M}, d^n, d^n)$.

2.1 The method: symmetry breaking in nonconvex optimization

In the realm of convexity, it is a nearly-trivial fact that the minimum of strictly convex invariant functions must be of full isotropy type. For nonconvex invariant functions however, matters are anything but trivial—no a-priori constraints on the isotropy type of minima exist. That said, somewhat miraculously, in various important settings critical points, and minima in particular, do exhibit large isotropy types. This phenomenon was first studied in [10], where it was shown that the $S_k \times S_d$ -isotropy groups of spurious minima corresponding to the ReLU kernel (11) tend to be large subgroups of the isotropy of global minimizers. Thus, intuitively, spurious minima break the symmetry of global minimizers, but not too much. Examples are provided in Figure 2. Based on this observation, families of critical points of \mathcal{L} were expressed as power series in $1/\sqrt{k}$ leading to, for example, a precise formula for the decay rate of \mathcal{L} [11]. The power series representation was then used in [12] to derive an analytic characterization of the Hessian spectrum of \mathcal{L} for finite arbitrarily large values of d and k . This access to precise high-dimensional spectral information allowed, for the first time, a rigorous examination of a number of fundamental hypotheses in the machine learning literature pertaining to curvature, optimization, and generalization.

3 Numerical results

Having presented the concept of symmetry breaking and its importance in studying nonconvex optimization landscapes, we now turn to explore various tensorial settings in which this principle applies. Our study is mainly based on numerical results, with the exception of a few simple cases in which we are able to perform exact calculations using the fact that \mathcal{L}_κ is a multivariate polynomial for polynomial kernels.

Experiment setting. In all experiments below, we initialize the entries of W as i.i.d. Gaussians with variance $1/d$ (commonly referred to as Xavier initialization) and run GD on problem (10) until the gradient norm is below a threshold of, unless stated otherwise, $1e-10$. Numerical values to 3 decimal points are provided in Section A (excluding spurious minima shown in Section 3.3). The gradient of (10) can be expressed as,

$$\nabla \mathcal{L}_\kappa(W) = \sum_{i=1}^k \mathbf{e}_i \otimes \left(\sum_{j=1}^k \kappa_{\mathbf{w}}(\mathbf{w}_i, \mathbf{w}_j) - \sum_{j=1}^h \kappa_{\mathbf{w}}(\mathbf{w}_i, \mathbf{v}_j) \right), \quad (16)$$

where $\kappa_{\mathbf{w}}$ denotes the derivative of κ with respect to the first argument and \mathbf{e}_i denotes the i -th unit vector. The weight matrices of convergent iterates are permuted so as to align with a $\Delta(S_{d_1} \times S_{d_2} \times \dots \times S_{d_p})$ -isotropy group where $d_1 \geq d_2 \geq \dots \geq d_p$. We numerically verify that the convergent iterates are indeed minima (i.e., the respective Hessian is positive semi-definite) using the following expressions for the Hessian entries,

$$\nabla^2 \mathcal{L}_\kappa(W) = \sum_{i,j=1}^k \mathbf{e}_i \mathbf{e}_j^\top \otimes \kappa_{\mathbf{w},\mathbf{v}}(\mathbf{w}_i, \mathbf{w}_j) + \sum_{i=1}^k \mathbf{e}_i \mathbf{e}_i^\top \otimes \left(\sum_{j=1}^k \kappa_{\mathbf{w},\mathbf{w}}(\mathbf{w}_i, \mathbf{w}_j) - \sum_{j=1}^h \kappa_{\mathbf{w},\mathbf{w}}(\mathbf{w}_i, \mathbf{v}_j) \right). \quad (17)$$

Note that, due to numerical errors, the Hessian is only guaranteed to be approximately positive semi-definite.

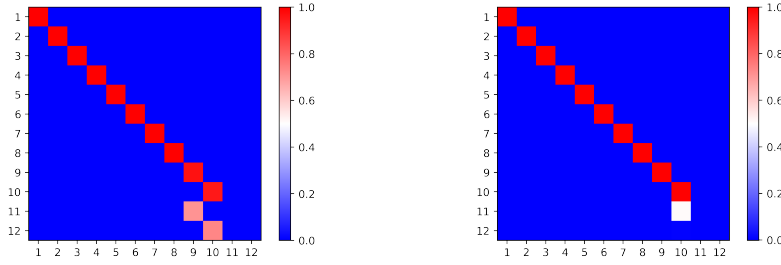


Figure 3: Spurious minima of optimization problem (1) instantiated with $d = k = 12$, order 5 symmetric tensors, the Frobenius norm (equivalently, the *quintic kernel* $\langle \cdot, \cdot \rangle^5$, as defined in (7)), and the target tensor $T = \sum_{i=1}^k \mathbf{e}_i^{\otimes 5}$. (Left) a spurious minimum of isotropy $\Delta(S_8 \times \langle (9\ 10)(11\ 12) \rangle)$ and function value 1. (Right) a spurious minimum of isotropy $\Delta(S_9 \times S_1^3)$ and of function value 1.

3.1 Identity target tensor

We start by studying the simple setting where one seeks a d -rank n -order tensor approximation for the d -rank identity tensor $T = \tau_n(I_d)$, with $d = 12$ and $n = 3, 5$. Following the procedure describe above, we obtain a number of symmetry breaking spurious minima for the polynomial kernel $k(\cdot, \cdot) = \langle \cdot, \cdot \rangle^r$ (representing the symmetric tensor decomposition problem (1)) for $r = 3$ and $r = 5$, shown in Figure 1 and Figure 3 respectively, and for the cubic-Gaussian kernel (15), shown in Figure 4.

3.2 Restricting the gradient equations to fixed point spaces

In contrast to the previous setting in which the phenomenon of symmetry breaking was studied, namely, problem (10) with the ReLU kernel (11), here the use of polynomial kernels yields a multivariate polynomial loss function. This makes it possible to rigorously establish various properties of symmetry breaking fixed point spaces using tools from computational algebra. We demonstrate this for $d = k$ over the cubic kernel and the identity target tensor.

$S_d \times S_d$ -critical points. We start by computing all the critical points of \mathcal{L} restricted to $M(d, d)^{S_d \times S_d} = \{\omega I_d \mid \omega \in \mathbb{R}\}$. To this end, we simply substitute the general form of W and note that

$$\begin{aligned} \mathcal{L}(\omega I) &= \omega^6 d^5 / 2 - \omega^3 d^2 + d/2, \\ \frac{d}{d\omega} \mathcal{L} &= 3\omega^5 d^5 - 3\omega^2 d^2. \end{aligned} \quad (18)$$

The simple polynomial gradient equation has two solutions $\omega = 0$ and $\omega = d^{-1}$. This, in turn, implies that the critical points of $\mathcal{L}|_{M(d, d)^{S_d \times S_d}}$ are $\mathbf{0}_d$ and $d^{-1}I_d$. In fact, due to the unique nature of fixed point spaces, \mathcal{L} and $\mathcal{L}|_{M(d, d)^{S_d \times S_d}}$ share the exact same set of $S_d \times S_d$ -critical points (see [10, Proposition 3]). Thus, we have a complete characterization of all the critical points of \mathcal{L} which are fixed by $S_d \times S_d$.⁵

⁵The fact that $W \in M(d, d)^{S_d \times S_d}$ is a critical point of $\nabla(\mathcal{L}|_{M(d, d)^{S_d \times S_d}})$ iff W is a critical point of $\nabla \mathcal{L}$ is also known as the *principle of symmetric criticality*. See [25] for a study of this principle in the context of G -manifolds, including cases where it fails to hold.

ΔS_d -critical points. Next, restricted to $M(d, d)^{\Delta S_d} = \{\omega_1 I_d + \omega_2(\mathbf{1}\mathbf{1}^\top - I_d) \mid \omega_1, \omega_2 \in \mathbb{R}\}$, the loss function \mathcal{L} reads

$$\begin{aligned} \mathcal{L}(\omega_1 I_d + \omega_2(\mathbf{1}\mathbf{1}^\top - I_d)) &= \omega_1^6 d/2 + \omega_1^4 \omega_2^2 (3d^2/2 - 3d/2) + \omega_1^3 \omega_2^3 (4d^2 - 4d) - \omega_1^3 d \\ &\quad + \omega_1^2 \omega_2^4 (15d^3/2 - 21d^2 + 27d/2) + \omega_1 \omega_2^5 (3d^4 - 15d^3 + 24d^2 - 12d) \\ &\quad + \omega_2^6 (d^5/2 - 3d^4 + 15d^3/2 - 17d^2/2 + 7d/2) + \omega_2^3 (-d^2 + d) + d/2, \end{aligned} \quad (19)$$

and the partial derivatives read

$$\begin{aligned} \frac{\partial}{\partial \omega_1} \mathcal{L} &= 3\omega_2^5 d^4 + d^3 (15\omega_1 \omega_2^4 - 15\omega_2^5) \\ &\quad + d^2 (6\omega_1^3 \omega_2^2 + 12\omega_1^2 \omega_2^3 - 42\omega_1 \omega_2^4 + 24\omega_2^5) \\ &\quad + d (3\omega_1^5 - 6\omega_1^3 \omega_2^2 - 12\omega_1^2 \omega_2^3 - 3\omega_1^2 + 27\omega_1 \omega_2^4 - 12\omega_2^5), \\ \frac{\partial}{\partial \omega_2} \mathcal{L} &= 3\omega_2^5 d^5 + d^4 (15\omega_1 \omega_2^4 - 18\omega_2^5) + d^3 (30\omega_1^2 \omega_2^3 - 75\omega_1 \omega_2^4 + 45\omega_2^5) \\ &\quad + d^2 (3\omega_1^4 \omega_2 + 12\omega_1^3 \omega_2^2 - 84\omega_1^2 \omega_2^3 + 120\omega_1 \omega_2^4 - 51\omega_2^5 - 3\omega_2^2) \\ &\quad + d (-3\omega_1^4 \omega_2 - 12\omega_1^3 \omega_2^2 + 54\omega_1^2 \omega_2^3 - 60\omega_1 \omega_2^4 + 21\omega_2^5 + 3\omega_2^2). \end{aligned} \quad (20)$$

Eliminating ω_1 using the lex-ordered Gröbner basis for the system of two polynomials (20) reveals that ω_2 must satisfy the following polynomial equation (see Section B for the complete specification of the corresponding Gröbner basis):

$$\begin{aligned} 0 &= \omega_2^{20} (d^{15} - 2d^{14}) \\ &\quad + \omega_2^{17} (36d^{12} - 248d^{11} + 480d^{10} - 256d^9) \\ &\quad + \omega_2^{14} (53d^{10} - 730d^9 + 3200d^8 - 5184d^7 + 2560d^6) \\ &\quad + \omega_2^{11} (15d^8 - 402d^7 + 3149d^6 - 11338d^5 + 17664d^4 - 9216d^3) \\ &\quad + \omega_2^8 (d^6 - 40d^5 + 535d^4 - 2735d^3 + 8388d^2 - 12960d + 6912) \\ &\quad + \omega_2^5 (-2d^3 + 25d^2 - 186d + 279) + \omega_2^2. \end{aligned} \quad (21)$$

Consequently, there exist at most 20 distinct values of the ω_2 -coordinate of critical points with isotropy equal or greater than ΔS_d . We defer further investigation of the restriction of the gradient equations to different fixed point spaces to future work.

3.3 Convolutional target tensor

In this section, we use convolutional target tensors to examine how symmetry breaking minima adapt to the isotropy of non-identity target tensors. We use the target tensor $T_{\text{Lap}} := \tau_3(V_{\text{Lap}})$ associated with the circulant *Laplacian-filter* matrix:

$$V_{\text{Lap}} := \begin{pmatrix} -2 & 1 & 0 & \cdots & 0 & 1 \\ & \ddots & & \ddots & & \\ & & & & & \\ 1 & 0 & \cdots & 0 & 1 & -2 \end{pmatrix}. \quad (22)$$

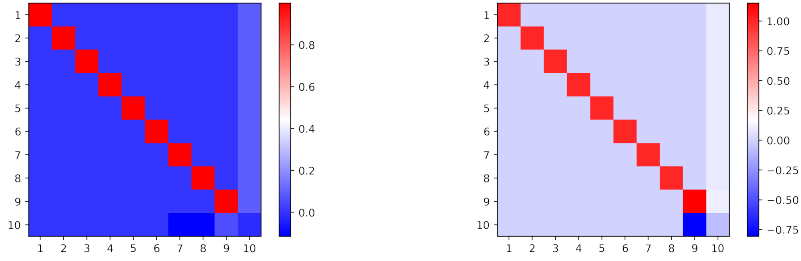


Figure 4: Spurious minima of optimization problem (1) instantiated with $d = k = 10$, order 3 symmetric tensors, the cubic-Gaussian kernel (15) and the target tensor $T = \sum_{i=1}^k \mathbf{e}_i^{\otimes 3}$. (Left) a spurious minimum of isotropy $\Delta(S_6 \times S_2 \times S_1^2)$ and function value 1. (Right) a spurious minimum of isotropy $\Delta(S_8 \times S_1^2)$ and function value 1.

The circulant structure of V_{Lap} is equivalent to a $\Delta\mathbb{Z}_d$ -isotropy which corresponds to convolutional filters used in state-of-the-art neural network architectures. Numerical experiments indicate that this choice of target tensor induces a very rugged ill-conditioned optimization landscape. In addition, the objective value corresponding to spurious minima in this model is typically higher compared to that of the identity target tensor. An example for a spurious minima for which the target tensor is T_{Lap} is given in Figure 5.

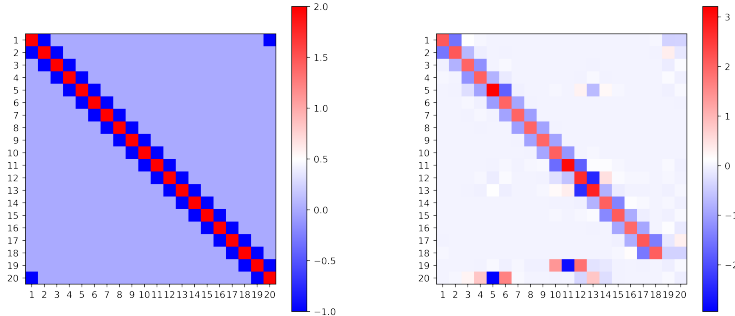


Figure 5: Spurious minima of optimization problem (1) instantiated with $d = k = 20$, order 3 symmetric tensors, the cubic kernel (7) and the Laplacian target tensor T_{Lap} . (Left) The target weight matrix V_{Lap} . (Right) a spurious minimum of function value ≈ 8.9 . Note that here the gradient norm is of the order of $1e-2$.

4 Conclusion

In this note, we showed that the principle of symmetry breaking minima, in which spurious minima break the symmetry of global minimizers, applies to symmetric tensor decomposition problems and kernel-like functions. This has several implications. First, nonconvex problems which exhibit this principle are amenable to a recently-developed set of symmetry-based tools [10, 11, 12] which, among others, provide an analytic characterization of families of critical points and local minima. This applies in particular to families of

spurious minima for tensor decomposition problems—a fundamental setting in machine learning. Secondly, we significantly extended the class of, otherwise perhaps episodic, nonconvex optimization problems in which the symmetry breaking principle had previously been observed. Thirdly, with the symmetry breaking principle now established for multivariate polynomials, it is the authors’ hope to obtain finer-grained results by using more tools from algebraic geometry.

Acknowledgments

Part of this work was performed while YA was visiting the Simons Institute for the Foundations of Deep Learning program. JB acknowledges partial support from the Alfred P. Sloan Foundation, NSF RI-1816753, NSF CAREER CIF 1845360, NSF CHS-1901091 and Samsung Electronics. JK acknowledges partial support from the Simons Collaboration in Algorithms and Geometry and start-up grants at UT Austin.

References

- [1] P. Comon, “Tensor decompositions,” *Mathematics in Signal Processing V*, pp. 1–24, 2002.
- [2] P. Comon and M. Rajih, “Blind identification of under-determined mixtures based on the characteristic function,” *Signal Processing*, vol. 86, no. 9, pp. 2271–2281, 2006.
- [3] L. De Lathauwer, B. De Moor, and J. Vandewalle, “A multilinear singular value decomposition,” *SIAM Journal on Matrix Analysis and Applications*, vol. 21, no. 4, pp. 1253–1278, 2000.
- [4] T. G. Kolda and B. W. Bader, “Tensor decompositions and applications,” *SIAM Review*, vol. 51, no. 3, pp. 455–500, 2009.
- [5] N. D. Sidiropoulos, R. Bro, and G. B. Giannakis, “Parallel factor analysis in sensor array processing,” *IEEE Transactions on Signal Processing*, vol. 48, no. 8, pp. 2377–2388, 2000.
- [6] A. Smilde, R. Bro, and P. Geladi, *Multi-Way Analysis: Applications in the Chemical Sciences*. John Wiley & Sons, 2005.
- [7] J. Landsberg, *Tensors: Geometry and Applications: Geometry and Applications*. Volume 128 of *Graduate Studies in Mathematics*, American Mathematical Society, 2011.
- [8] A. Choromanska, M. Henaff, M. Mathieu, G. B. Arous, and Y. LeCun, “The loss surfaces of multilayer networks,” in *Artificial intelligence and statistics*, pp. 192–204, PMLR, 2015.
- [9] V. Ros, G. B. Arous, G. Biroli, and C. Cammarota, “Complex energy landscapes in spiked-tensor and simple glassy models: Ruggedness, arrangements of local minima, and phase transitions,” *Physical Review X*, vol. 9, no. 1, p. 011003, 2019.
- [10] Y. Arjevani and M. Field, “On the principle of least symmetry breaking in shallow ReLU models,” *arXiv preprint arXiv:1912.11939*, 2019.
- [11] Y. Arjevani and M. Field, “Symmetry and critical points for a model shallow neural network,” *CoRR*, vol. abs/2003.10576, 2020.

- [12] Y. Arjevani and M. Field, “Analytic characterization of the hessian in shallow ReLU models: a tale of symmetry,” *arXiv preprint arXiv:2008.01805*, 2020.
- [13] T. G. Kolda, “Numerical optimization for symmetric tensor decomposition,” *Mathematical Programming*, vol. 151, no. 1, pp. 225–248, 2015.
- [14] N. Vervliet, O. Debals, L. Sorber, M. Van Barel, and L. De Lathauwer *Tensorlab 3.0*, Available online, Mar. 2016.
- [15] B. W. Bader, T. G. Kolda, *et al. Tensor Toolbox for MATLAB, Version 3.2*, www.tensortoolbox.org, February 10, 2021.
- [16] J. Nie, “Generating polynomials and symmetric tensor decompositions,” *Foundations of Computational Mathematics*, vol. 17, no. 2, pp. 423–465, 2017.
- [17] “Foundations of the PARAFAC procedure: models and conditions for an “explanatory” multimodal factor analysis,” *UCLA Working Papers in Phonetics*, vol. 16, pp. 1–84, 1970.
- [18] L. De Lathauwer, J. Castaing, and J.-F. Cardoso, “Fourth-order cumulant-based blind identification of underdetermined mixtures,” *IEEE Transactions on Signal Processing*, vol. 55, no. 6, pp. 2965–2973, 2007.
- [19] S. B. Hopkins, T. Schramm, and J. Shi, “A robust spectral algorithm for overcomplete tensor decomposition,” in *Conference on Learning Theory*, pp. 1683–1722, PMLR, 2019.
- [20] J. Kileel and J. M. Pereira, “Subspace power method for symmetric tensor decomposition and generalized PCA,” *arXiv preprint arXiv:1912.04007*, 2019.
- [21] S. Sherman and T. G. Kolda, “Estimating higher-order moments using symmetric tensor decomposition,” *SIAM Journal on Matrix Analysis and Applications*, vol. 41, no. 3, pp. 1369–1387, 2020.
- [22] M. J. Field, *Dynamics and Symmetry*, vol. 3 of *ICP Advanced Texts in Mathematics*. Imperial College Press, London, 2007.
- [23] A. Rahimi, B. Recht, *et al.*, “Random features for large-scale kernel machines.,” in *NIPS*, vol. 3, p. 5, Citeseer, 2007.
- [24] Y. Arjevani, J. Bruna, J. Kileel, and M. Trager, “Geometry and optimization of shallow polynomial networks,” *In-preparation*, 2021.
- [25] R. S. Palais, “The principle of symmetric criticality,” *Communications in Mathematical Physics*, vol. 69, no. 1, pp. 19–30, 1979.

A Numerics of spurious minima

Numerics of spurious minima presented in the body of the note are indicated by colors to convey the overall structure of the symmetry in a compact visual manner. Here we provide the numerical values of the entries to 3 decimal places.

1.000e+00	2.009e-31	8.100e-31	-9.491e-32	1.395e-31	-6.311e-32	5.576e-31	-2.851e-31	-1.173e-31	-7.345e-25	-7.452e-25	-2.546e-32
1.454e-31	1.000e+00	4.240e-31	-4.968e-32	7.302e-32	-3.303e-32	2.919e-31	-1.493e-31	-6.141e-32	-3.845e-25	-3.901e-25	-1.332e-32
2.363e-30	1.709e-30	1.000e+00	-8.074e-31	1.187e-30	-5.369e-31	4.744e-30	-2.426e-30	-9.981e-31	-6.249e-24	-6.340e-24	-2.166e-31
3.244e-32	2.347e-32	9.461e-32	1.000e+00	1.629e-32	-7.371e-33	6.513e-32	-3.331e-32	-1.370e-32	-8.580e-26	-8.704e-26	-2.973e-33
7.007e-32	5.070e-32	2.044e-31	-2.395e-32	1.000e+00	-1.592e-32	1.407e-31	-7.195e-32	-2.960e-32	-1.853e-25	-1.880e-25	-6.423e-33
1.434e-32	1.038e-32	4.183e-32	-4.901e-33	7.204e-33	1.000e+00	2.880e-32	-1.473e-32	-6.059e-33	-3.793e-26	-3.848e-26	-1.315e-33
1.120e-30	8.101e-31	3.266e-30	-3.827e-31	5.625e-31	-2.545e-31	1.000e+00	-1.150e-30	-4.731e-31	-2.962e-24	-3.005e-24	-1.026e-31
2.928e-31	2.118e-31	8.540e-31	-1.001e-31	1.471e-31	-6.654e-32	5.879e-31	1.000e+00	-1.237e-31	-7.744e-25	-7.856e-25	-2.684e-32
4.956e-32	3.586e-32	1.446e-31	-1.694e-32	2.490e-32	-1.126e-32	9.952e-32	-5.089e-32	1.000e+00	-1.311e-25	-1.330e-25	-4.543e-33
3.230e-17	2.337e-17	9.422e-17	-1.104e-17	1.623e-17	-7.341e-18	6.487e-17	-3.317e-17	-1.365e-17	9.748e-01	-8.685e-02	-2.961e-18
3.305e-17	2.391e-17	9.639e-17	-1.129e-17	1.660e-17	-7.510e-18	6.636e-17	-3.393e-17	-1.396e-17	-8.757e-02	9.741e-01	-3.029e-18
-2.005e-16	-1.451e-16	-5.848e-16	6.852e-17	-1.007e-16	4.556e-17	-4.026e-16	2.059e-16	8.470e-17	4.206e-01	4.244e-01	1.838e-17

Table 1: The spurious minimum on the left hand side of Figure 1.

1.000e+00	1.098e-22	4.259e-21	-3.654e-20	2.654e-22	6.967e-22	6.027e-22	2.093e-22	1.455e-22	-1.387e-22	1.608e-15	-2.983e-24
3.707e-23	1.000e+00	4.855e-22	-4.162e-21	3.025e-23	7.940e-23	6.869e-23	2.385e-23	1.658e-23	-1.580e-23	1.832e-16	-3.390e-25
5.486e-20	1.852e-20	1.000e+00	-6.412e-18	4.477e-20	1.175e-19	1.016e-19	3.531e-20	2.454e-20	-2.339e-20	2.840e-13	-4.342e-22
-1.223e-19	-4.120e-20	-2.008e-18	1.000e+00	-9.970e-20	-2.638e-19	-2.277e-19	-7.858e-20	-5.459e-20	5.204e-20	-6.082e-11	4.477e-21
2.165e-22	7.311e-23	2.836e-21	-2.433e-20	1.000e+00	4.639e-22	4.013e-22	1.393e-22	9.685e-23	-9.233e-23	1.071e-15	-1.984e-24
1.492e-21	5.038e-22	1.954e-20	-1.682e-19	1.218e-21	1.000e+00	2.766e-21	9.604e-22	6.675e-22	-6.363e-22	7.405e-15	-1.384e-23
1.117e-21	3.770e-22	1.462e-20	-1.258e-19	9.113e-22	2.392e-21	1.000e+00	7.187e-22	4.995e-22	-4.762e-22	5.535e-15	-1.032e-23
1.347e-22	4.546e-23	1.764e-21	-1.513e-20	1.099e-22	2.885e-22	2.496e-22	1.000e+00	6.023e-23	-5.742e-23	6.657e-16	-1.233e-24
6.506e-23	2.196e-23	8.521e-22	-7.306e-21	5.309e-23	1.394e-22	1.206e-22	4.187e-23	1.000e+00	-2.774e-23	3.215e-16	-5.952e-25
5.912e-23	1.996e-23	7.744e-22	-6.639e-21	4.824e-23	1.267e-22	1.096e-22	3.804e-23	2.644e-23	1.000e+00	2.922e-16	-5.407e-25
-2.238e-09	-7.552e-10	-2.983e-08	1.770e-06	-1.826e-09	-4.802e-09	-4.152e-09	-1.440e-09	-1.001e-09	9.538e-10	9.838e-01	5.892e-12
1.646e-08	5.557e-09	2.195e-07	-1.302e-05	1.343e-08	3.533e-08	3.055e-08	1.059e-08	7.362e-09	-7.018e-09	3.627e-01	-4.335e-11

Table 2: The spurious minimum on the right hand side of Figure 1.

1.000e+00	1.136e-23	1.990e-23	-1.290e-23	-3.186e-23	-2.958e-23	1.030e-23	-1.989e-23	3.365e-21	2.418e-21	-6.478e-24	4.943e-25
3.793e-23	1.000e+00	7.762e-23	-6.754e-23	-1.347e-22	-1.327e-22	3.981e-23	-7.762e-23	1.325e-20	-1.802e-23	-3.101e-23	-3.020e-23
1.707e-22	2.404e-22	1.000e+00	-3.053e-22	-6.084e-22	-5.997e-22	1.797e-22	-3.504e-22	5.982e-20	-2.958e-22	-1.401e-22	-1.371e-22
1.001e-22	1.379e-22	2.020e-22	1.000e+00	-3.500e-22	-3.444e-22	1.036e-22	-2.020e-22	3.448e-20	5.469e-22	-8.035e-23	-7.659e-23
1.552e-21	2.185e-21	3.185e-21	-2.775e-21	1.000e+00	-5.450e-21	1.633e-21	-3.185e-21	5.437e-19	-2.617e-21	-1.274e-21	-1.246e-21
1.466e-21	2.061e-21	3.006e-21	-2.618e-21	-5.218e-21	1.000e+00	1.542e-21	-3.006e-21	5.131e-19	-1.882e-21	-1.202e-21	-1.174e-21
1.181e-23	1.663e-23	2.425e-23	-2.113e-23	-4.210e-23	-4.149e-23	1.000e+00	-2.425e-23	4.139e-21	-2.046e-23	-9.697e-24	-9.486e-24
1.707e-22	2.404e-22	3.504e-22	-3.053e-22	-6.084e-22	-5.997e-22	1.797e-22	1.000e+00	5.982e-20	-2.958e-22	-1.401e-22	-1.371e-22
-1.507e-06	-2.122e-06	-3.092e-06	2.695e-06	5.369e-06	5.292e-06	-1.586e-06	3.092e-06	9.613e-01	2.610e-06	1.237e-06	1.210e-06
-1.674e-06	6.256e-07	-4.628e-08	-1.233e-06	-6.927e-07	-1.206e-06	-4.986e-08	4.360e-08	1.400e-06	9.524e-01	-4.065e-07	-2.357e-06
5.091e-06	7.170e-06	1.045e-05	-9.106e-06	-1.815e-05	-1.789e-05	5.360e-06	-1.045e-05	7.090e-01	-8.820e-06	-4.180e-06	-4.089e-06
4.682e-06	-1.750e-06	1.294e-07	3.450e-06	1.937e-06	3.372e-06	1.395e-07	-1.220e-07	-3.915e-06	7.364e-01	1.137e-06	6.591e-06

Table 3: The spurious minimum on the left hand side of Figure 3.

1.000e+00	1.449e-15	3.861e-16	-1.585e-16	1.132e-16	-5.812e-16	1.261e-15	4.187e-17	-4.238e-16	-4.633e-15	2.454e-17	-1.822e-18
-3.312e-15	1.000e+00	6.434e-16	1.774e-16	-7.934e-16	-1.922e-15	-2.667e-16	-2.715e-16	-8.504e-16	-3.463e-14	2.905e-19	1.035e-17
-1.702e-17	1.342e-17	1.000e+00	4.827e-19	-3.381e-18	-9.949e-18	8.241e-19	-1.151e-18	-4.744e-18	-1.720e-16	-2.455e-20	5.234e-20
1.445e-18	-3.934e-18	-1.008e-18	1.000e+00	-8.703e-19	9.594e-19	-4.897e-18	-3.091e-19	1.022e-18	-5.431e-18	-1.161e-19	1.601e-20
4.777e-18	-1.015e-17	-2.597e-18	1.465e-18	1.000e+00	3.047e-18	-1.130e-17	-5.900e-19	2.720e-18	1.525e-18	-2.889e-19	3.508e-20
-1.355e-16	2.035e-16	5.417e-17	-2.143e-17	1.408e-17	1.000e+00	1.731e-16	5.249e-18	-5.973e-17	-6.960e-16	3.422e-18	-2.378e-19
2.496e-15	-8.916e-15	-2.318e-15	1.755e-15	-2.466e-15	1.754e-15	1.000e+00	-8.722e-16	2.282e-15	-2.281e-14	-2.479e-16	3.856e-17
7.674e-20	-1.641e-19	-4.205e-20	2.387e-20	-2.703e-20	4.901e-20	-1.834e-19	1.000e+00	4.399e-20	1.802e-20	-4.643e-21	5.664e-22
-2.959e-17	3.162e-17	8.550e-18	-1.302e-18	-2.404e-18	-1.764e-17	1.574e-17	-7.791e-19	1.000e+00	-2.403e-16	2.889e-19	3.244e-20
1.643e-07	-3.081e-07	-8.977e-08	5.072e-08	-5.718e-08	1.052e-07	-3.214e-07	-2.046e-08	9.400e-08	9.932e-01	-7.092e-07	-1.114e-08
-2.415e-06	4.528e-06	1.319e-06	-7.454e-07	8.403e-07	-1.545e-06	4.724e-06	3.007e-07	-1.381e-06	5.073e-01	1.042e-05	1.638e-07
1.038e-03	-1.760e-03	-4.700e-04	2.209e-04	-2.000e-04	6.472e-04	-1.672e-03	-7.257e-05	5.068e-04	4.054e-03	-3.043e-05	2.839e-06

Table 4: The spurious minimum on the right hand side of Figure 3.

9.989e-01	-5.396e-04	-5.396e-04	-5.396e-04	-5.396e-04	-5.396e-04	-5.386e-04	-5.386e-04	-5.386e-04	-5.386e-04	9.208e-02
-5.396e-04	9.989e-01	-5.396e-04	-5.396e-04	-5.396e-04	-5.396e-04	-5.386e-04	-5.386e-04	-5.386e-04	-5.386e-04	9.208e-02
-5.396e-04	-5.396e-04	9.989e-01	-5.396e-04	-5.396e-04	-5.396e-04	-5.386e-04	-5.386e-04	-5.386e-04	-5.386e-04	9.208e-02
-5.396e-04	-5.396e-04	-5.396e-04	9.989e-01	-5.396e-04	-5.396e-04	-5.386e-04	-5.386e-04	-5.386e-04	-5.386e-04	9.208e-02
-5.396e-04	-5.396e-04	-5.396e-04	-5.396e-04	9.989e-01	-5.396e-04	-5.386e-04	-5.386e-04	-5.386e-04	-5.386e-04	9.208e-02
-5.404e-04	-5.404e-04	-5.404e-04	-5.404e-04	-5.404e-04	9.995e-01	9.689e-04	-1.312e-03	-1.312e-03	9.221e-02	9.221e-02
-5.404e-04	-5.404e-04	-5.404e-04	-5.404e-04	-5.404e-04	-5.404e-04	9.995e-01	9.689e-04	-1.312e-03	9.221e-02	9.221e-02
-5.401e-04	-5.401e-04	-5.401e-04	-5.401e-04	-5.401e-04	-5.401e-04	-1.719e-04	9.989e-01	9.989e-01	9.216e-02	9.216e-02
9.324e-05	9.324e-05	9.324e-05	9.324e-05	9.324e-05	9.324e-05	-1.149e-01	-1.149e-01	5.752e-02	-1.591e-02	-1.591e-02

Table 5: The spurious minimum on the left hand side of Figure 4.

9.989e-01	-5.397e-04	-5.397e-04	-5.397e-04	-5.397e-04	-5.397e-04	-5.397e-04	-5.397e-04	-5.397e-04	-5.397e-04	9.209e-02
-5.397e-04	9.989e-01	-5.397e-04	-5.397e-04	-5.397e-04	-5.397e-04	-5.397e-04	-5.397e-04	-5.397e-04	-5.397e-04	9.209e-02
-5.397e-04	-5.397e-04	9.989e-01	-5.397e-04	-5.397e-04	-5.397e-04	-5.397e-04	-5.397e-04	-5.397e-04	-5.397e-04	9.209e-02
-5.397e-04	-5.397e-04	-5.397e-04	9.989e-01	-5.397e-04	-5.397e-04	-5.397e-04	-5.397e-04	-5.397e-04	-5.397e-04	9.209e-02
-5.397e-04	-5.397e-04	-5.397e-04	-5.397e-04	9.989e-01	-5.397e-04	-5.397e-04	-5.397e-04	-5.397e-04	-5.397e-04	9.209e-02
-5.397e-04	-5.397e-04	-5.397e-04	-5.397e-04	-5.397e-04	9.989e-01	9.989e-01	9.989e-01	9.989e-01	9.989e-01	9.209e-02
-6.214e-04	-6.214e-04	-6.214e-04	-6.214e-04	-6.214e-04	-6.214e-04	-6.214e-04	-6.214e-04	-6.214e-04	-6.214e-04	1.060e-01
4.358e-04	4.358e-04	4.358e-04	4.358e-04	4.358e-04	4.358e-04	4.358e-04	4.358e-04	4.358e-04	-8.066e-01	-7.436e-02

Table 6: The spurious minimum on the right hand side of Figure 4.

B Gröbner basis for the system of gradient equations restricted to $M(d, d)^{\Delta S_d}$

$$\begin{aligned}
 \mathfrak{g} = & \left\{ \begin{aligned}
 & \omega_1^2(\omega_1^2 - 11\omega_1^6 + 446\omega_1^8 + 1772\omega_1^{10} - 39011\omega_1^{12} + 469078\omega_1^{14} - 4254514\omega_1^{16} + 246191321\omega_1^{18} - 15248402213\omega_1^{20} + 6021967468\omega_1^{22} + 2630185298\omega_1^{24} - 21104018744\omega_1^{26} - 6776767564\omega_1^{28} + 20825048100) \\
 & + \omega_1^2(-\omega_1^2 + 27\omega_1^6 + 27\omega_1^8 - 4662\omega_1^{10} + 3732\omega_1^{12} + 30610\omega_1^{14} - 680788\omega_1^{16} + 42241132\omega_1^{18} - 1528482213\omega_1^{20} - 6021967468\omega_1^{22} + 15248402213\omega_1^{24} - 21104018744\omega_1^{26} - 6776767564\omega_1^{28} + 20825048100) \\
 & + \omega_1^2(-10\omega_1^6 - 3238\omega_1^8 + 7283\omega_1^{10} - 236810\omega_1^{12} + 236810\omega_1^{14} - 3567228\omega_1^{16} + 23385325\omega_1^{18} - 930133265\omega_1^{20} + 2814837016\omega_1^{22} - 5781835872\omega_1^{24} + 8317273150\omega_1^{26} + 5410331376\omega_1^{28} - 21801317864\omega_1^{30} + 30758253184\omega_1^{32}) \\
 & + \omega_1^2(78\omega_1^6 - 1715\omega_1^8 + 156001\omega_1^{10} - 869273\omega_1^{12} - 10166713\omega_1^{14} - 283846224\omega_1^{16} + 11803011328\omega_1^{18} - 83302923716\omega_1^{20} + 310477492824\omega_1^{22} - 83302923716\omega_1^{24} + 11803011328\omega_1^{26} - 283846224\omega_1^{28} - 10166713\omega_1^{30} + 156001\omega_1^{32}) \\
 & + \omega_1^2(10\omega_1^6 + 333\omega_1^8 + 3732\omega_1^{10} + 1230178\omega_1^{12} + 25884818\omega_1^{14} + 2000310331\omega_1^{16} + 2000310331\omega_1^{18} + 25884818\omega_1^{20} + 1230178\omega_1^{22} + 3732\omega_1^{24} + 333\omega_1^{26} + 10\omega_1^{28}) \\
 & + \omega_1^2(\omega_1^6 + 33\omega_1^8 - 3889\omega_1^{10} + 128413\omega_1^{12} + 1284389\omega_1^{14} - 3900138\omega_1^{16} - 81110833\omega_1^{18} + 7864572353\omega_1^{20} - 44014825224\omega_1^{22} + 147133594464\omega_1^{24} - 30454830132\omega_1^{26} + 29181833332\omega_1^{28} - 38494830636) \\
 & + \omega_1^2(16\omega_1^6 - 510\omega_1^8 + 1492\omega_1^{10} - 3732\omega_1^{12} - 200124\omega_1^{14} + 680088\omega_1^{16} - 12254122\omega_1^{18} + 102102718\omega_1^{20} - 1591021321\omega_1^{22} + 12734937576\omega_1^{24} + 1052306480) \\
 & + \omega_1^2(-15\omega_1^6 - 510\omega_1^8 + 30048\omega_1^{10} - 817113\omega_1^{12} + 1310949\omega_1^{14} - 4320194\omega_1^{16} + 3304800\omega_1^{18} - 18901212\omega_1^{20} + 42047128\omega_1^{22} - 10734937576\omega_1^{24} + 1052306480) \\
 & + \omega_1^2(4\omega_1^6 + 2042\omega_1^8 - 180333\omega_1^{10} + 207123\omega_1^{12} - 10157010\omega_1^{14} - 8834183291\omega_1^{16} + 8572846131\omega_1^{18} + 45399541235\omega_1^{20} - 1390825011711\omega_1^{22} - 413187310890\omega_1^{24} + 2190884107496\omega_1^{26} + 2190884107496\omega_1^{28} - 413187310890\omega_1^{30} + 1390825011711\omega_1^{32} - 8572846131\omega_1^{34} + 8834183291\omega_1^{36} - 10157010\omega_1^{38} + 207123\omega_1^{40} - 2042\omega_1^{42} + 4\omega_1^{44}) \\
 & + \omega_1^2(-\omega_1^6 + 3010\omega_1^8 - 47061\omega_1^{10} + 2270973\omega_1^{12} - 4878783\omega_1^{14} + 57171719\omega_1^{16} - 35149792\omega_1^{18} + 16178810767\omega_1^{20} - 78487481481\omega_1^{22} + 253032035728\omega_1^{24} - 643011685954\omega_1^{26} + 12304157628268\omega_1^{28} - 181585608573171\omega_1^{30} + 201313821488100\omega_1^{32} - 29102825182824\omega_1^{34} + 4418865261084\omega_1^{36} \\
 & + \omega_1^2(10\omega_1^6 - 7912\omega_1^8 + 63185\omega_1^{10} - 3524338\omega_1^{12} + 12828303\omega_1^{14} - 633729017\omega_1^{16} + 291107815\omega_1^{18} + 10975824721\omega_1^{20} - 29604657024\omega_1^{22} - 154251312424\omega_1^{24} + 647227273016\omega_1^{26} - 2038133146343\omega_1^{28} + 9432828376967\omega_1^{30} - 18468741552256\omega_1^{32} + 38184516562828\omega_1^{34} - 8774672000996\omega_1^{36} - 6123214747578\omega_1^{38} + 21084625896768 - 33131171294170) \\
 & + \omega_1^2(-10\omega_1^6 + 1607\omega_1^8 + 1607\omega_1^{10} - 125913\omega_1^{12} + 125913\omega_1^{14} - 15904979\omega_1^{16} + 15904979\omega_1^{18} - 18708113\omega_1^{20} + 891411092\omega_1^{22} - 477048128\omega_1^{24} - 3074985780\omega_1^{26} + 14713288222\omega_1^{28} - 30928295513\omega_1^{30} + 14713288222\omega_1^{32} - 3074985780\omega_1^{34} + 15904979\omega_1^{36} - 125913\omega_1^{38} + 1607\omega_1^{40} - 1607\omega_1^{42} + 10\omega_1^{44}) \\
 & + \omega_1^2(\omega_1^6 - 11\omega_1^8 + 4162\omega_1^{10} - 2776\omega_1^{12} + 200124\omega_1^{14} + 680088\omega_1^{16} - 12254122\omega_1^{18} + 102102718\omega_1^{20} - 1591021321\omega_1^{22} + 12734937576\omega_1^{24} + 1052306480) \\
 & + \omega_1^2(\omega_1^6 - 24\omega_1^8 + 1405\omega_1^{10} - 3928\omega_1^{12} + 5335\omega_1^{14} - 6910\omega_1^{16} + 7233661\omega_1^{18} - 21190105\omega_1^{20} - 481107692\omega_1^{22} + 103590909\omega_1^{24} + 192238400\omega_1^{26} - 190483737\omega_1^{28} + 6779030672\omega_1^{30} - 1873738985\omega_1^{32}) \\
 & + \omega_1^2(5\omega_1^6 - 1038\omega_1^8 + 2609\omega_1^{10} - 184820\omega_1^{12} + 2965073\omega_1^{14} - 38382229\omega_1^{16} + 82520943\omega_1^{18} - 916209413\omega_1^{20} - 1326574510\omega_1^{22} - 3022587424\omega_1^{24} + 5100157218226\omega_1^{26} - 621302823032\omega_1^{28} + 544535001818\omega_1^{30} - 31703100188\omega_1^{32} + 110765096131\omega_1^{34} - 1726545278\omega_1^{36}) \\
 & + \omega_1^2(5\omega_1^6 - 131\omega_1^8 + 843\omega_1^{10} - 28035\omega_1^{12} + 51163\omega_1^{14} - 692822\omega_1^{16} + 3215117\omega_1^{18} - 28090403\omega_1^{20} + 2427203032\omega_1^{22} - 1920772309\omega_1^{24} + 163832232\omega_1^{26} + 7083010326\omega_1^{28} - 360247110\omega_1^{30} + 33701079110\omega_1^{32} - 13201079110\omega_1^{34} + 13201079110\omega_1^{36} - 360247110\omega_1^{38} + 7083010326\omega_1^{40} - 163832232\omega_1^{42} + 1920772309\omega_1^{44} - 2427203032\omega_1^{46} + 3215117\omega_1^{48} - 51163\omega_1^{50} + 131\omega_1^{52} - 843\omega_1^{54} + 28035\omega_1^{56} - 843\omega_1^{58} + 131\omega_1^{60} - 5\omega_1^{62} + 5\omega_1^{64}) \\
 & + \omega_1^2(\omega_1^6 + 29\omega_1^8 + 840\omega_1^{10} + 28884\omega_1^{12} + 423403\omega_1^{14} + 423403\omega_1^{16} - 3008310\omega_1^{18} + 101433093\omega_1^{20} + 1244804902\omega_1^{22} + 20825025016\omega_1^{24} - 3008310\omega_1^{26} + 101433093\omega_1^{28} - 101433093\omega_1^{30} + 3008310\omega_1^{32} - 423403\omega_1^{34} - 423403\omega_1^{36} - 28884\omega_1^{38} - 840\omega_1^{40} - 29\omega_1^{42} + \omega_1^{44}) \\
 & + \omega_1^2(\omega_1^6 + 23\omega_1^8 - 338\omega_1^{10} + 31768\omega_1^{12} + 105215\omega_1^{14} - 15110218\omega_1^{16} + 2600393\omega_1^{18} + 28953315\omega_1^{20} - 583125071\omega_1^{22} + 7294925412\omega_1^{24} - 168500137031\omega_1^{26} + 2728781537260\omega_1^{28} - 2950187948570\omega_1^{30} - 944571041728\omega_1^{32} + 19031007261) \\
 & + \omega_1^2(\omega_1^6 - 2\omega_1^8 + 2\omega_1^{10} + \omega_1^{12}(\omega_1^6 + 356\omega_1^8 - 238\omega_1^{10} + 320\omega_1^{12} - 138\omega_1^{14} + 176\omega_1^{16} - 92\omega_1^{18} - 4\omega_1^{20} - 8\omega_1^{22} + 4\omega_1^{24} + 25\omega_1^{26} - 186\omega_1^{28} + 279) + \omega_1^{24}) \\
 \end{aligned} \right.$$